ON THE ACOUSTICS OF SHOCKS GENERATED BY THE RUPTURE OF DIAPHRAGMS IN A TUBE

T. C. BHADRA*

NATIONAL CENTER FOR ATMOSPHERIC RESEARCH, BOULDER, COLORADO

(*Received September* 20, 1966)

ABSTRACT. The results are presented of the analysis of oscillograms due to shocks generated by the rupture of diaphragms in a shock tube. Shock overpressures p_o and the duration t_o of ceiling pressure to zero level transit have been determined from the oscillograms as functions of compression chamber pressures and distances. Shock velocities have been determined by the time of arrival method. The values of shock overpressures as determined by these two methods agree satisfactorily.

INTRODUCTION

Reiman (1880) and Hugoniot (1887) have already very early theoretically demonstrated that a pressure wave of finite amplitude changes its form during the propagation in such a manner that its front becomes increasingly steeper and its end increasingly flatter. A shock wave is characterized by a relatively large change in excess pressure across a very small region of space. Such shocks can result from explosions like the rupture of a membrane separating a region of high pressure from a region of low pressure in a tube or from a detonation of chemical explosives.

The literature on shock waves is extensive (Courant *et al.*, 1948) and here we shall content ourselves with the analysis of the pressure oscillograms of shock waves generated by breaking the diaphragm separating high and low pressure regions in a tube. The short duration of the shock makes an analysis of the direct measurements rather difficult, so that the analytical evaluation of the Furrer integral from the oscillograms has been pursued. In this respect the work of Furrer (1946) is an outstanding contribution to the physics and mathematics of explosions due to TNT explosives, cannon shot, and pistol shot. Leonard (1962) briefly discussed his work in a review article on explosive sound sources. In the present investigation, the method used by Furrer to analyse the pressure oscillograms due to the above mentioned explosions will be followed to analyse the pressure oscillograms due to the shock generated in a tube by the rupture of the membrane. Here no attempt has been made to introduce a correction term in the pressure distribution along the axis of the tube due to reflection, because of the complex mathematics involved to compute the reflection term. This is partly due to the irregular inside structure of the shock tube.

*Permanent address: Bose Institute, 93/1 Upper Circular Road, Calcutta 9, India.

In order to gain a clear insight into the physical characteristics of a shock, it is important to know the chronological sequence of the atmospheric pressure and its speed of propagation. The shock overpressure was measured by means of a calibrated piezoelectric transducer made by Kistler company, and speed of propagation was measured by the time of arrival method.

II. THEORETICAL CONSIDERATIONS

The most essential characteristics of a shock are the sudden onset and the short duration. In the case of a shock due to explosion, we have to expect a virtually discontinuous pressure leap. The parameters decisive for the effect of an explosion thrust, especially the pressure leap and the air speed, can be traced back to a single parameter, the wave velocity. In the vicinity of the explosion site, where the pressure leap and the air speed are high, the velocity of a wave is also very high. With increasing distance it approaches the velocity of sound asymptotically. As opposed to classical sound relationship a difference results in that the speed of propagation is no longer a pure material constant and the step pressure is added to the hydrostatic pressure, but these differences disappear very rapidly.

CHRONOLOGICAL PRESSURE DISTRIBUTION

In order to study the common form of the chronological pressure distribution of a shock in a cylindrical enclosure the following simple function which has been used by Furrer to study explosive waves in open atmosphere will be employed to analyse the pressure oscillograms in the present investigations :

$$p_t = p_0/\cos\theta e^{-bt}\cos(\Omega t+\theta) \qquad \ldots (1)$$

where p_0, the pressure ceiling, and t_0, the duration of the pressure ceiling up to zero transit, will be introduced as two parameters from the oscillograms. Equation (1) has been found to fit the experimental shock tube data satisfactorily.

The following boundary conditions are to be satisfied for the determinations of b, Ω, and θ from the magnitude of p_0 and t_0.

1. The chronological integral must be zero, i.e., physically the elastical procedure will be assumed and there will be no gas transport.

$$\int_0^\infty p_t dt = \frac{p_0}{\cos\theta}\int_0^\infty e^{-bt}\cos(\Omega t+\theta)dt = 0 \qquad \ldots (2)$$

i.e.,
$$\int_0^\infty e^{-bt}\cos(\Omega t+\theta)dt = 0 \qquad \ldots (3)$$

which leads to $tg\theta = \frac{b}{\Omega}$ ... (4)

$$\text{The maximum of} \quad F(p_t) = \frac{p_{0'}}{2b} \text{ , when } \omega^2 = \Omega^2 + b^2 \qquad (12)$$

The shock itself can be interpreted as the sum of infinitely many vibrations with the assigned amplitudes of the Fourier integral

$$p_t = \frac{1}{2\pi} \int_{-\infty}^{+\infty} e^{jwt} F(p_t) d\omega \qquad \ldots (13)$$

APPARATUS

Figure *I(a)* shows the photographs of the experimental arrangements and Figure 1(b) shows the schematic diagram of the shock tube in which the shocks were generated by rupturing AVISCO Cellophane Type 195 MSBO diaphragms with a metallic pointer activated by a solenoid. The number of sheets required

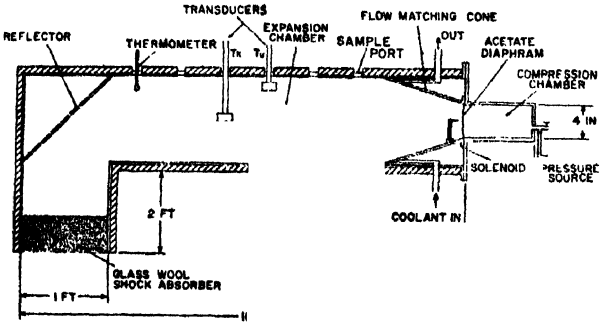

Fig. 1(b) : Schematic diagram of the shock tube.

depends upon the ratio of the pressures on the two sides of the diaphragms. A minimum of 3, 5, and 8 sheets are required for the corresponding pressure ratios of 1.045, 1.758, and 3.515 (15, 25, and 50 psi). Air is used both for the driving and the driven gas. The flow of the gas from the compression chamber after the rupture of the membrane is matched by introducing a metallic cone 91.44 cms.long (3 feet) in between the compression and the expansion chambers. A pressure gauge is coupled to the compression chamber to read the air pressure in it.

The expansion chamber containing air at atmospheric pressure is cooled to about $-10°C$ by circulating coolant from a constant temperature bath through a coil system incorporated in the chamber. The ratio of the cross-sectional areas of the compression and the expansion chambers is 3. Sample ports and observation windows are provided in the expansion chamber. The reflection of shock waves from the end of the expansion chamber is minimized with the help of a perforated acoustic reflector fixed at an angle of 45° to the axis of the shock tube assembly and a pad of glass wool enclosing the end of the tube. The outside of the expansion chamber is wrapped with a thick lining of glass wool in order to reduce heat transfer.

A calibrated quartz transducer T_k Model No. 601*A*, its associated electrostatic charge amplifier Model 566 made by the Kistler Instrument Corporation and a Tektronix Type 545A oscilloscope are used to measure the shock overpressure. The natural frequency and the rise time of the transducer are 140kc/s and 3 μ secs., respectively.

A second transducer T_g, made by Gulton Industries, and a H/P-400H VTVM are used in addition to the transducer, T_k, to measure the shock speed by the time of arrival method.

For further details about the shock tube and the results obtained on the interactions of shock waves with supercooled water (0 5 to 1 cc.) contained in glass and tygon tubings and with a single suspended supercooled droplet, reference is made to the papers by Goyer, Bhadra, and Gitlin (1965) and Bhadra (1965).

EXPERIMENTS

In order to understand the mechanism of the interaction of shock waves with supercooled water, experiments were carried out to determine the following shock parameters as functions of distance and compression chamber pressure : (*i*) chronological pressure distribution, p_t, (ii) speed of shock wave, U_s, (iii) acoustic energy, W, (iv) frequency spectrum, $F(p_t)$.

The chronological pressure distribution was determined by means of the transducer T_k in conjunction with the charge amplifier and the Tektronix oscilloscope. The oscilloscope was triggered by the signal picked up by the transducer, T_g, from the shock field. The transducer, T_g, was located ahead of the pressure amplitude measuring transducer, T_k, at a known distance from it. The transducer, T_g, was inserted into the shock field in such a way that the flow pattern in front of the transducer, T_k, was not disturbed to an appreciable amount. So the transducer T_g, was placed far off from the axial region as is shown in Figure 1. The axes of the transducers were aligned parallel to the direction of the gas flow.

The sensitivity of the transducer, T_k, is 1.0 $\mu\mu$ Cb/psi and the charge amplifier is calibrated in terms of mv/$\mu\mu$ Cb.

From the oscillogram, the magnitude of the peak overpressure, p_0, and the time, T, taken by the shock wave to travel the distance, D, between the two transducers, T_k and T_g, were estimated. The shock speed was determined from the measured values of the time, T, and the distance, D. P_0 and T where measured as functions of the compression chamber pressure and the distance from the diaphragm. Another parameter, t_0, the time for the ceiling pressure to return to zero transit region was determined from the oscillogram. These values of p_0 and t_0 are used in determining the chronological pressure distribution, p_t, acoustic energy, W, and the frequency spectrum, $F(p_t)$.

RESULTS AND DISCUSSIONS

Figures 2(a) and 2(b) show the two typical oscillograms of 3.515 Kg/cm² compression chamber pressure at distances 2.44 *m* and 1.83 m respectively. The

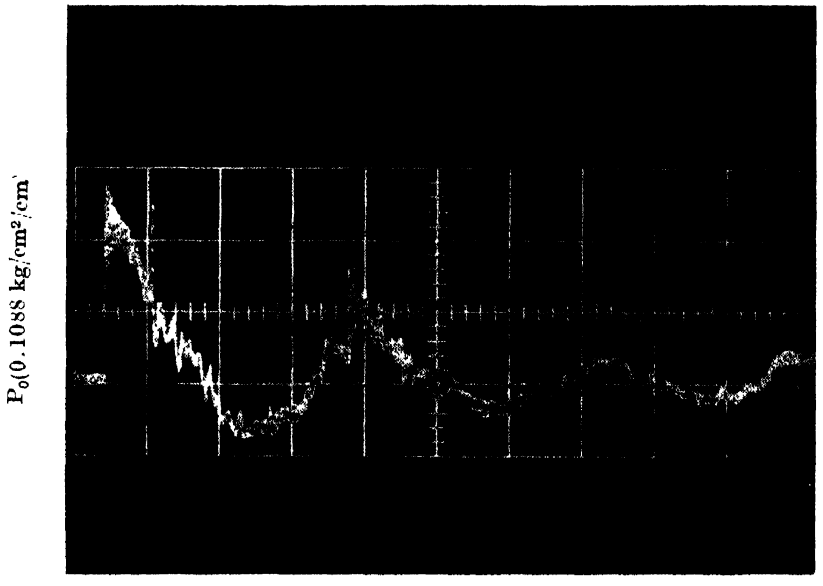

Time → 2ms/division (Large)

Fig. 2: Pressure oscillogram of 3.515 Kg/cm² compression chamber pressure. Ordinate: p_0 in 0.1088 Kg/cm²/cm. Abscissa: (a) Time in 2 ms/cm. at a distance of 2.44m.

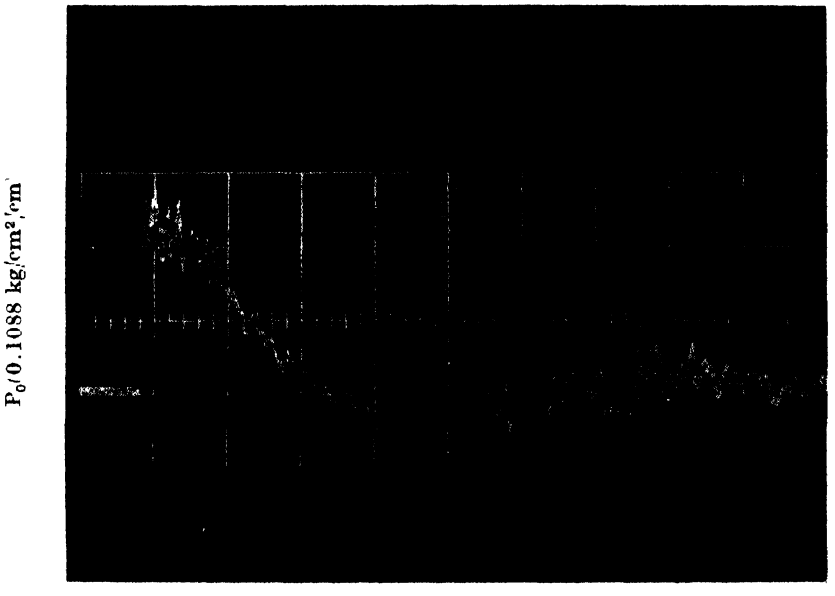

Time → 1ms/division (Large)

(b) Time in 1 ms/cm at a distance of 1.83m.

measured values of p_0, the ceiling pressure, t_0, the duration of the ceilingg pressure up to zero leve lransition, U_x, the shock velocity, and the calculated valves of W_1 the acoustic energy, p_c, the shock overpressuro, M_x, the mach number, are presented in the table as functions of distance and compression chamber pressnro. The velocity of sound in dry air at $-10°C$ is 326 m/s. Column 'c' of the table shows the measured ceiling pressure, p_0 and Column 'd' shows the same as calculated from the ratio of shock velocity and sound velocity. The overall agreement between the measured and the calculated ceiling pressures is fairly satisfactorp, but for 3.515 kg/cm^2 compression chamber pressure, the agreement is excellent Column 'f' shows an appreciable increase of the shock velocities over the sound velocity at $-10°C$ as shown in Column 'g'. Column 'i' shows the amount of acoustic energy/cm^2 available for each compression chamber pressure at different distances. Column 'h' shows the maximum value of the mach number using the minimum value of sound velocity. No correction for moisture content in air has been added.

For the pressure 3.515 Kg/cm^2 a minimum number of 8 diaphragms is required. However, at compression chamber pressures of 1.758 Kg/cm^2/and 1.045 Kg/cm^2 diaphragms cannot be ruptured by the metallic pointer so that 5 and 3 diaphragms are used respectively for these two cases. Since the number of diaphragms is changed when the compression chamber pressure is changed, it is difficult to relate correctly the ceiling pressure to the compression chamber pressure, but repeated experiments under similar conditions produced almost identical oscillograms.

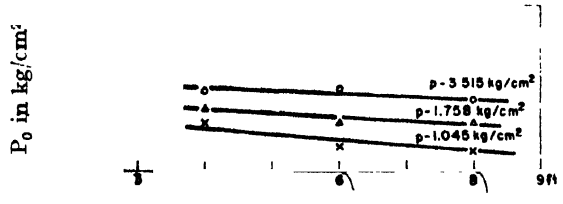

Fig. 3 : $p_0 \rightarrow$Overpressure plotted against distance as a function of the chamber pressure.

Figure 3 shows the measured ceiling pressure, p_0, at various distances. p_0 decreases inversely with distance up to 1.22 m. It was not possible to measure the ceilling pressures at smaller distances, i.e., less than 1.22 m In these regions the plots of p_0 against distance are shown by dashed lines indicating the uncertainty of the inverse relationship.

In Figure 4, the measured values of t_0 and p_0 are shown dependent on the compression chamber pressure. The measured values of t_0 from the oscillograms for compression chamber pressures of 1.758 Kg/cm^2 and 1.045 Kg/cm^2 at a distance of 1.22m have been found to be much smaller than those at 1.83m and 2.44m. The curve for t_0 against compression chamber pressure is steeper indicating, thereby, the rapid leveling down of the shock overpressure. In the region of 1.22m

the shock profile builds up and therefore it is difficult to visualise the mechanism involved for the lower values of t_0.

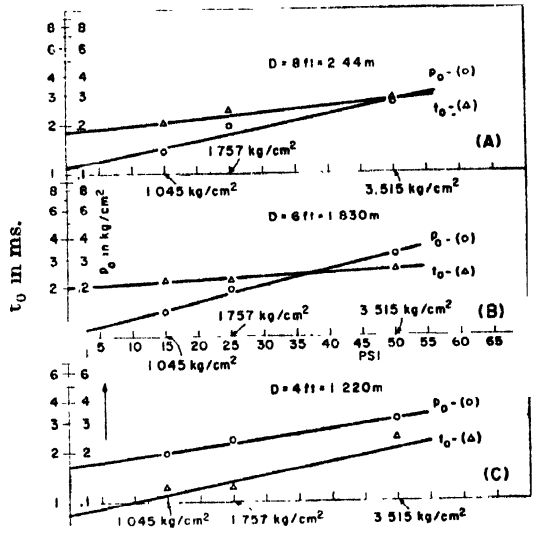

Fig. 4 : p_0 and t_0 are plotted against the pressure in the compression chamber.

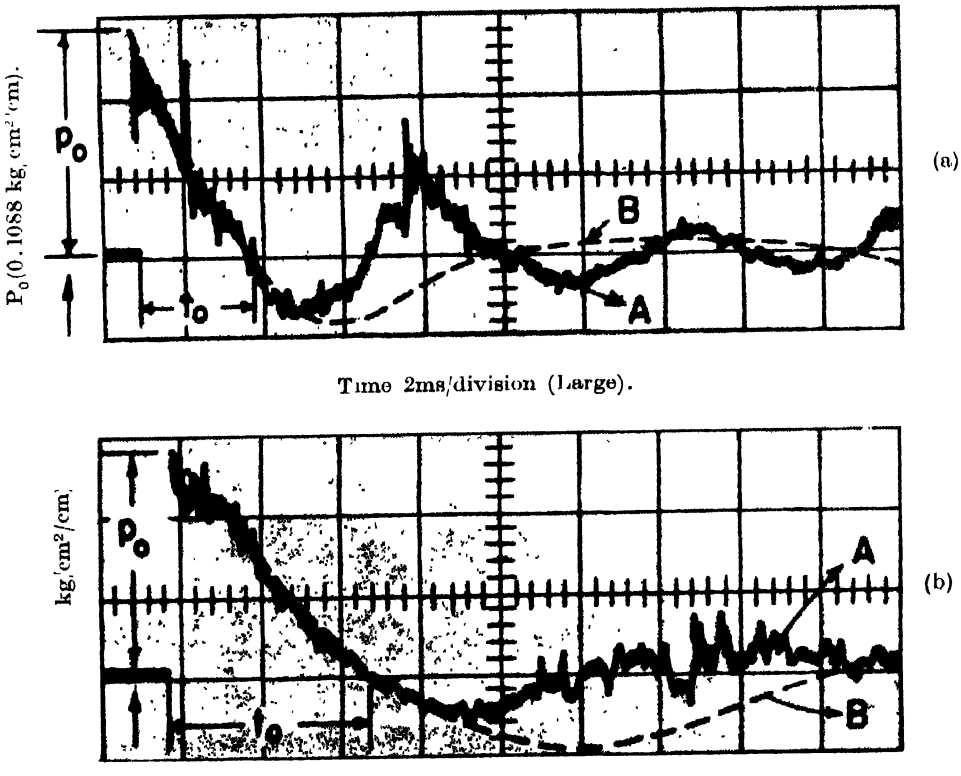

Fig. 5 : Approximate function of the shock oscillogram of 3.515/Kg/cm² compression chamber pressure. (a) at 2.44 meter, (b) at 1.83 meter.

TABLE I
Results

Serial No.	*a in meters	b in Kg/cm²	c Kg/cm²	d Kg/cm²	e in milli-sec.	f meter/ sec	g meter/ sec	h M_x	i in watts
1	1.22	3.515	0.305	0.374	2.4	373.99	326	1.15	0.0173
2	1.22	1.758	0.231	0.319	1.2	366.62	326	1.13	0.0050
3	1.22	1.045	0.196	0.218	1.2	356.22	326	1.09	0.0033
4	1.83	3.515	0.316	0.347	2.5	372.16	326	1.14	0.0193
5	1.83	1.758	0.196	0.245	2.2	358.75	326	1.10	0.0061
6	1.83	1.045	0.141	0.218	2.2	354.48	326	1.09	0.0029
7	2.44	3.515	0.267	0.272	2.8	363.02	326	1.11	0.0160
8	2.44	1.758	0.231	0.170	2.4	350.22	326	1.07	0.0067
9	2.44	1.045	0.196	0.143	2.2	345.95	326	1.06	0.0026

*a distance from the diaphragm

b compression chamber pressure

c measured shock ceiling overpressure p_0

d shock ceiling overpressure p_c calculated from ratios of shock velocity U_x and sound velocity a_x

e duration of pressure ceiling up to zero level transition t_0

f shock velocity U_x as measured by time of arrival method

g sound velocity a_x in dry air at —10°C, velocity of sound increases by 0.05 m/s for addition of 0.10% by volume of moisture (in the present case air is not free from moisture).

h m_x the mach number $= f/g = \frac{U_x}{a_x}$

i acoustic energy W in watts/unit area

In Figure 5, only two typical oscillograms of 3.515 Kg/cm² compression chamber pressure at 2.44m and 1.83m are represented by the curves A on which the curves B representing the approximate function

$$p_t = \frac{p_0}{\cos\theta} e^{-bt} \cos\ (\Omega t + \theta)$$

are superimposed. These curves present fairly good agreement between the theoretical and experimental values without correcting the theoretical values for reflection.

Figure 6 shows the frequency spectrum of the sound pulse from the shocks as calculated approximately from Fourier transform of the Equation (1). The Fourier transform is represented by Equation (10). In the figure, pressure amplitudes per 1 c.p.s. (*Hz*) at a distance of 2.44m for the compression chamber pressures of 3.515 Kg/cm², 1.758 Kg/cm², and 1.045 Kg/cm² are represented by the curves A, B, and C. The ordinate represents the pressure amplitudes in decibel/Hz. The 0 *db* has been defined to be equal to 1 $\mu b/Hz$. The maximum pressure amplitude is given by Equation (12). The pressure amplitude falls to zero at zero

frequency. The peak in the spectrums moves towards the lower frequency side of the spectrum as the pressure in the compression chamber is increased. This peak frequency, however, has no relationship whatsoever to the acoustical resonance frequency of the shock tube. For the three different cases, the peak frequencies are 454 Hz, 530Hz, and 636Hz for the compression chamber pressures of 3.515 Kg/cm², 1.758 Kg/cm², and 1.945 Kg/cm², respectively.

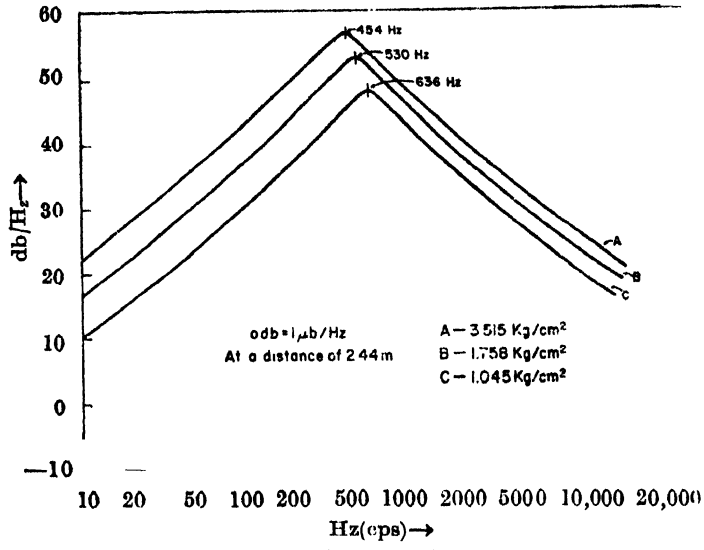

Fig. 6 : Frequency spectrum as a function of compression chamber pressure.

Figure 7 represents sound pulse amplitude distribution as a function of frequencies at different distances for one compression chamber pressure. The pressure amplitudes of lower frequencies are higher at larger distances. The findings are in agreement with the theory of shock waves, i.e., shock waves decay into low frequency sound waves at larger distances.

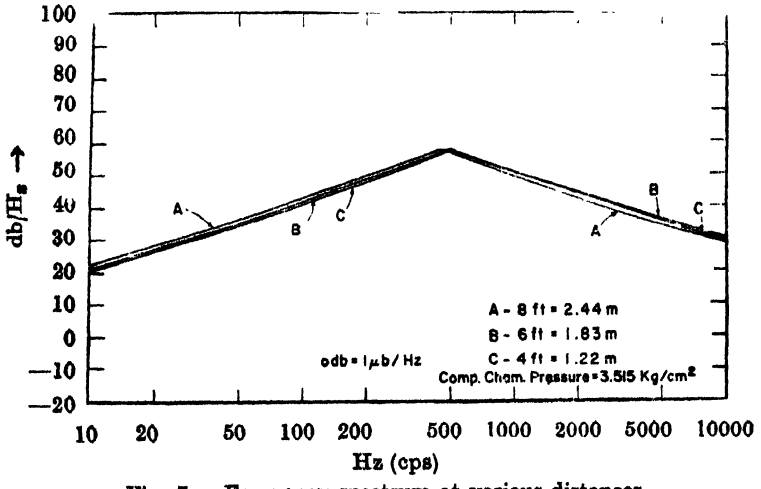

Fig. 7 : Frequency spectrum at various distances.

CONCLUSION

It may be concluded here that Equation (1) can be used satisfactorily to analyze the shock tube data. Further, this analysis provides data in elucidating the mechanism involved to trigger freezing of supercooled water by shock waves for which this shock tube is designed.

ACKNOWLEDGMENT

The author expresses his sincere thanks to Dr. G. G. Goyer and Dr. Y Nagakawa of NCAR and to Prof. R. W. Leonard, Physics Department, UCLA, for their valuable discussions and suggestions.

REFERENCES

Bhadra, T. C. (to be published.)

Bradley, J. N., 1962, *Shock Waves in Chemistry and Physics*, John Wiley and Sons, Inc., N.Y.

Courant, R. and Friedrichs, K. O., 1948, *Supersonic Flow and Shock Waves*, Interscience Publishers, Inc., N.Y.

Furrer, W., 1946 *Schweizer Arch. Angew. Wiss. Techn.*, **12**, 213.

Furrer, W., and Weber, H., 1946, *Tehn. Mit. Schwiez, Telegr. U.* Telph.—Verio No. 6.

Goyer, G. G., Bhadra, T. C. and Gitlin, S., 1965, *J. Applied Meteor.*, **4**, 156.

Hugoniot, H., 1887, *Journ. del' ecole Polytechn.*, Paris, 57.

Leonard, R. W., 1962, *Handbuch Der Physik by S. Flugge*, Akustik II, Springer-Verlag, Berlin.

Reiman, B., Nachr. Ges. Wiss, 1880, *Goltingen*, 8.